# Supporting Information

## A Porous Sodalite-Type MOF Based on Tetrazolcarboxylate Ligand and $[Cu_4Cl]^{7+}$ Square with Open Metal Sites for Gas Sorption

Dongmei Wang, Tingting Zhao, Guanghua Li, Qisheng Huo and Yunling Liu*

*State Key Laboratory of Inorganic Synthesis and Preparative Chemistry, College of Chemistry, Jilin University, Changchun 130012, P. R. China*

**Experimental procedures and analytical data for JLU-Liu2:**

Preparation of **JLU-Liu2**: Under solvothermal conditions, $CuCl_2 \cdot 2H_2O$ (0.0136 g, 0.08 mmol), 4-(1H-tetrazol-5-yl)-benzoic acid ($H_2TBA$, 0.0076 mg, 0.04 mmol), EtOH (1 mL), and DMF (1 mL), was sealed in a 20 mL vial and heated at 65 ºC for 3d, and then cooled to room temperature. The green truncated octahedron-shaped crystals were collected and air-dried (73% yield based on $CuCl_2 \cdot 3H_2O$). Crystal data for **JLU-Liu2**: $[H_3O][(Cu_4Cl)(TBA)_4(H_2O)_4] \cdot 2DMF \cdot 3H_2O$, Cubic, space group $Pm$-3m, $a$ = 20.208(2) Å, V = 8252.0(16) Å$^3$, Z = 3, Final R indicates [$I > 2\sigma(I)$]: $R_1$ = 0.0736, $wR_2$ = 0.2069. Elemental analysis (wt%): Calcd for $C_{38}H_{47}ClCu_4N_{18}O_{18}$: C 34.2, H 3.50, N 18.9. found: C 33.7, H 3.42, N 18.1.

**Fig. S1.** Optical image of **JLU-Liu2** crystals.

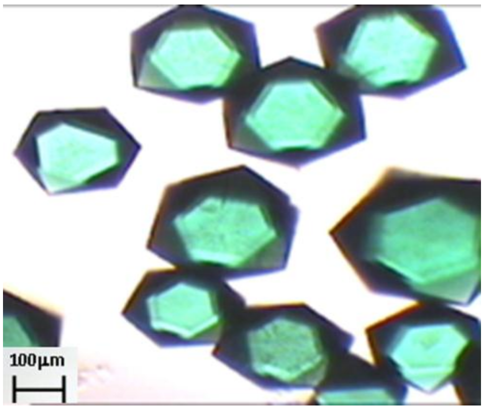

**Fig. S2.** Infrared spectra for **JLU-Liu2** (4000-400 cm$^{-1}$).

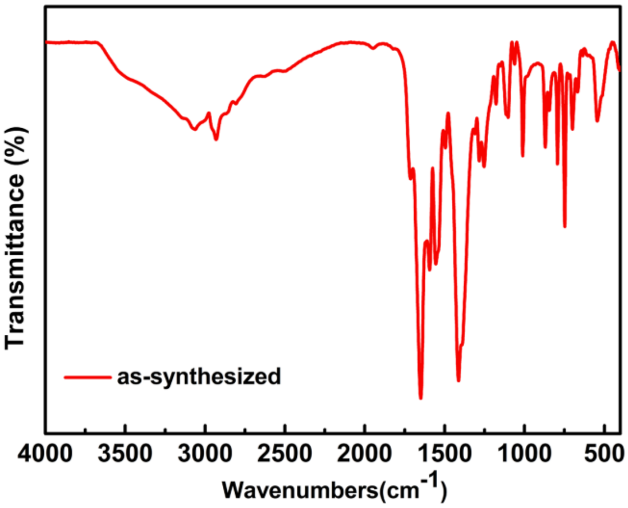

**Fig. S3.** Experimental and calculated powder X-ray diffraction (PXRD) patterns for **JLU-Liu2**, indicating the phase purity of the as-synthesized samples.

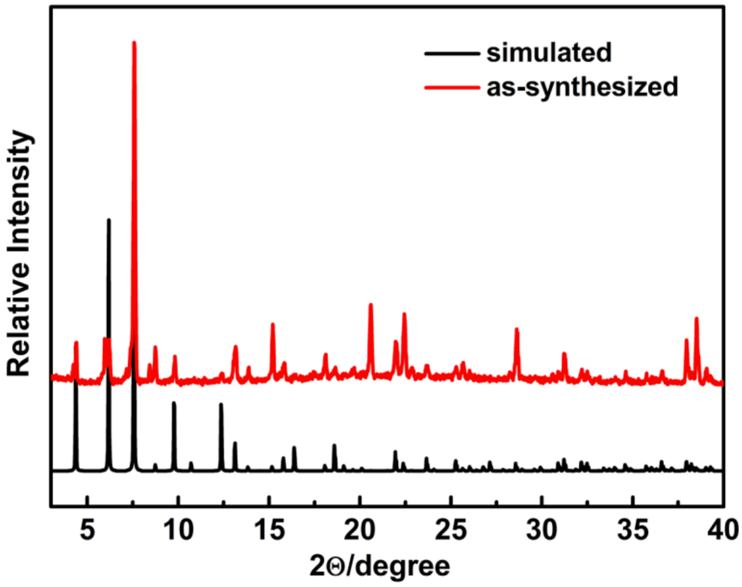

**Fig. S4**. The TGA curves of **JLU-Liu2** and exchanged by MeOH.

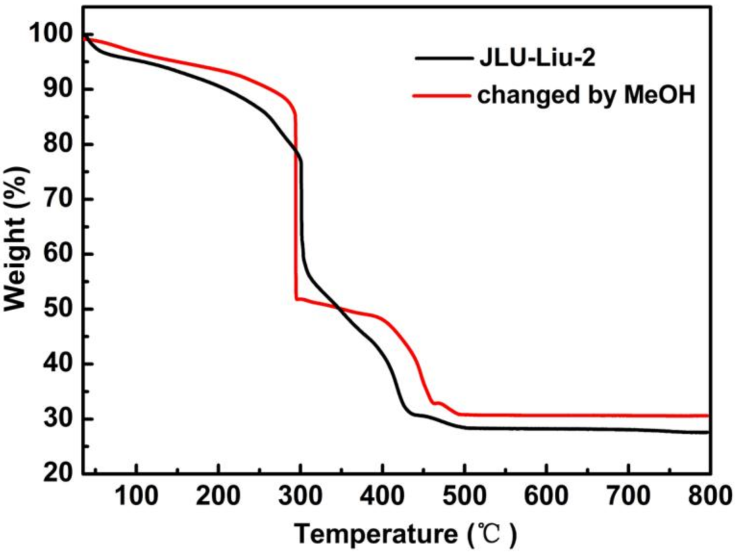

Thermogravimetric analysis (TGA) for the as-synthesized **JLU-Liu2** sample shows a weight loss of 21 % (calcd: 21.8 %) between 35 and 286 $^{o}$C, corresponding to the loss of three $H_2O$ molecules, two DMF molecules, four coordination $H_2O$ and one $H_3O^+$. On further heating, two-step weight loss of 53 % between 286 and 430 $^{o}$C should be corresponding to the release of the organic $TBA^{2-}$ ligand (calcd: 54.3 %). XRD studies indicated that the final product, upon calcinations above 600 $^{o}$C, is a pure dense CuO phase (JCPDS: 45-0937).

**Fig. S5.** (a) Three types of [Cu$_4$Cl]$^{7+}$ SBUs constructed by tetrazol and/or carboxylate group. (b) TBA$^{2-}$ ligand can be regarded as linear node. (c) Polyhedral view of the framework of **JLU-Liu2** with reo topology.

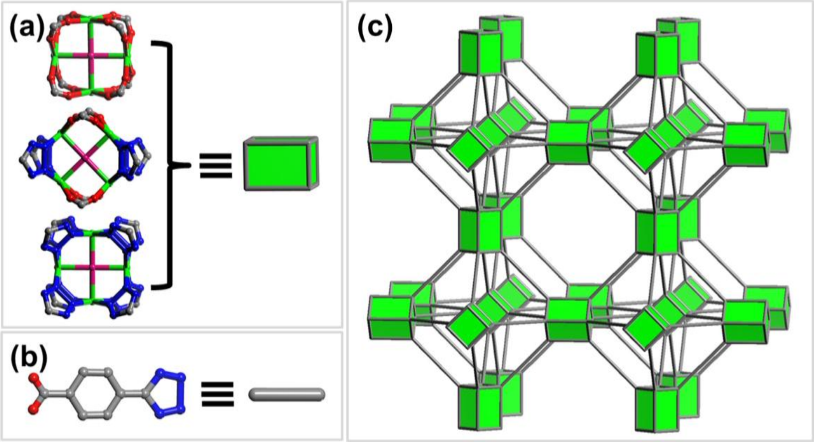

**Fig. S6.** (a) The [Cu$_4$Cl]$^{7+}$ square SBU defined by four Cu$^{2+}$ ions and a Cl$^-$ anion. (b) Reported sodalite-like MOFs constructed by different ligands (H$_3$BTC,[1,2] H$_3$BTT,[3] H$_3$BTTri,[4,5] H$_3$TTCA,[6] H$_3$TPB-3tz,[7] H$_3$TPT-3tz[7]), which can be regarded as a triangle node. (c) The reported sodalite-like MOFs based on small SOD cage with different sizes. (d) The reported sodalite-like MOFs containing big SOD cage with different sizes. Color code: Cu, green; O, red; C, gray; N, blue. (Hydrogen atoms and guest molecules have been omitted for clarity).

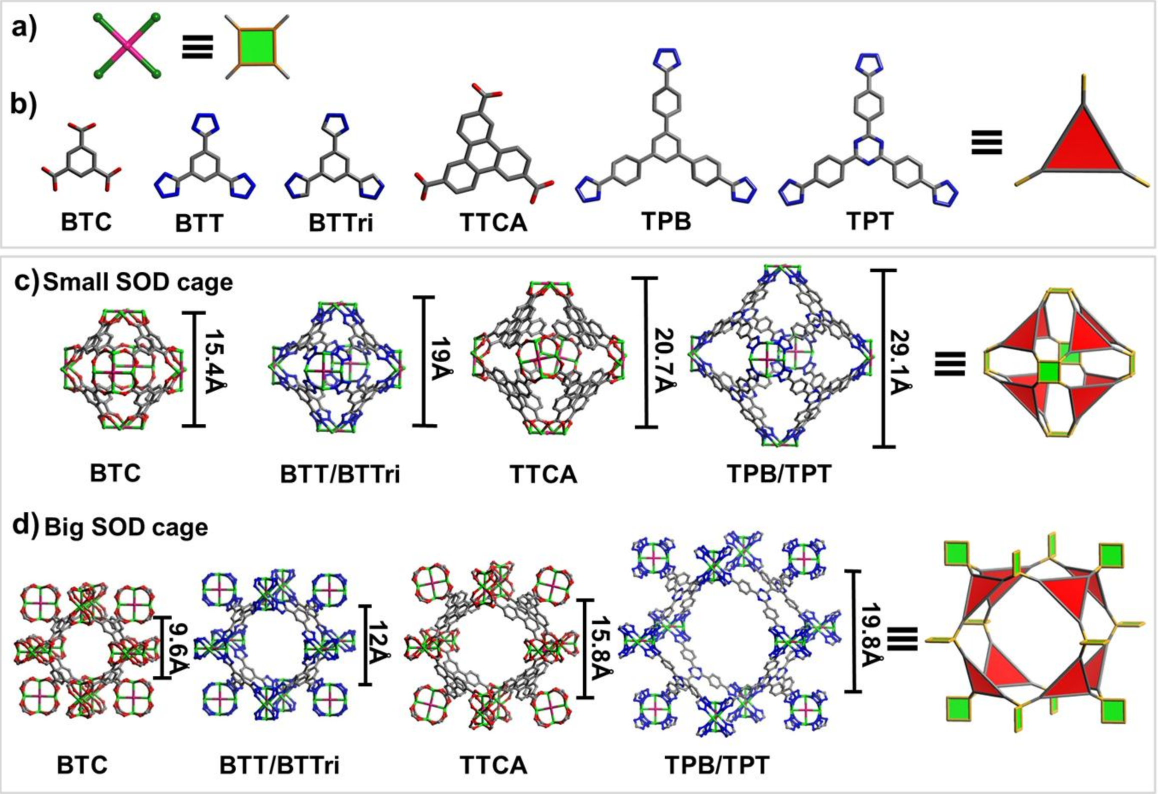

**Fig. S7.** Comparison of the construction of SOD cage reported in sodalite-like MOFs and this work. Reported work[1-6] (The structures having the ligands on the face of the polyhedral): the small sodalite-like cage consisted of 8 triangle ligands and 6 squares, and the big sodalite-like cage built by 8 triangle ligands and 12 squares, formulated as $[Cu_4Cl]_6L_8$ and $[Cu_4Cl]_{12}L_8$, respectively. However, in present work (The structure having the ligand on the edge, as compared to having them on the face of the polyhedron, is a quite significant advance to construct a edge-decorated polyhedral framework): the small sodalite-like cage based on 12 linear ligands and 6 squares and the big sodalite-like cage constructed by 24 linear ligands and 12 squares, formulated as $[Cu_4Cl]_6L_{12}$ and $[Cu_4Cl]_{12}L_{24}$, respectively.

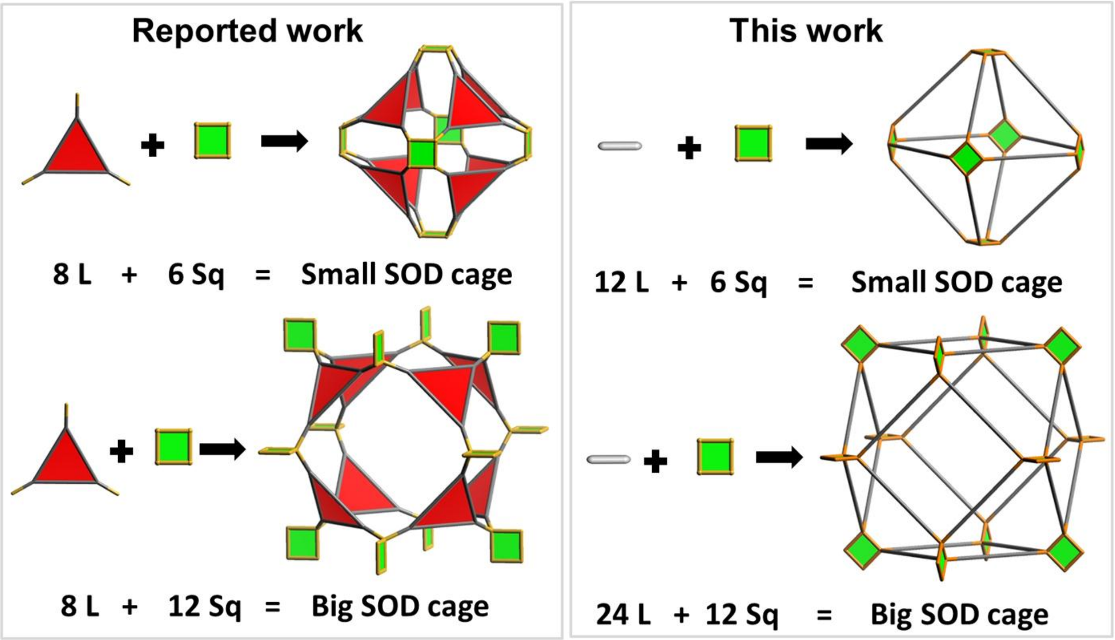

**Fig. S8**. Nitrogen sorption isotherms on **JLU-Liu2** at 77 K and pore size distribution analysis. Adsorption and desorption branches are shown with closed and open symbols, respectively.

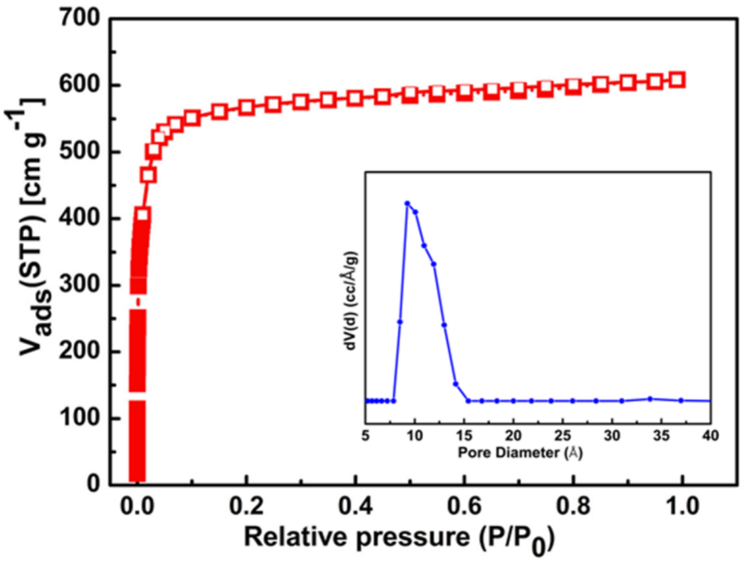

**Fig. S9.** (a) Hydrogen adsorption isotherm of **JLU-Liu2** at 77 K (red) and 87 K (blue). Adsorption and desorption branches are shown with closed and open symbols, respectively. (b) Isosteric heat of adsorption of $H_2$ in **JLU-Liu2**.

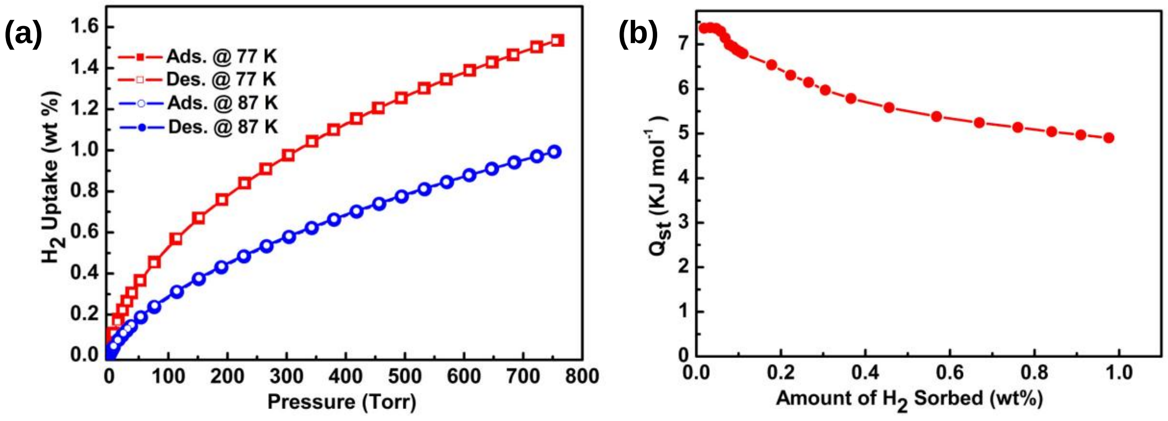

**Fig. S10.** (a) Carbon dioxide adsorption isotherm of **JLU-Liu2** at 273 K (red) and 298 K (blue). Adsorption and desorption branches are shown with closed and open symbols, respectively. (b) Isosteric heat of adsorption of $H_2$ in **JLU-Liu2**.

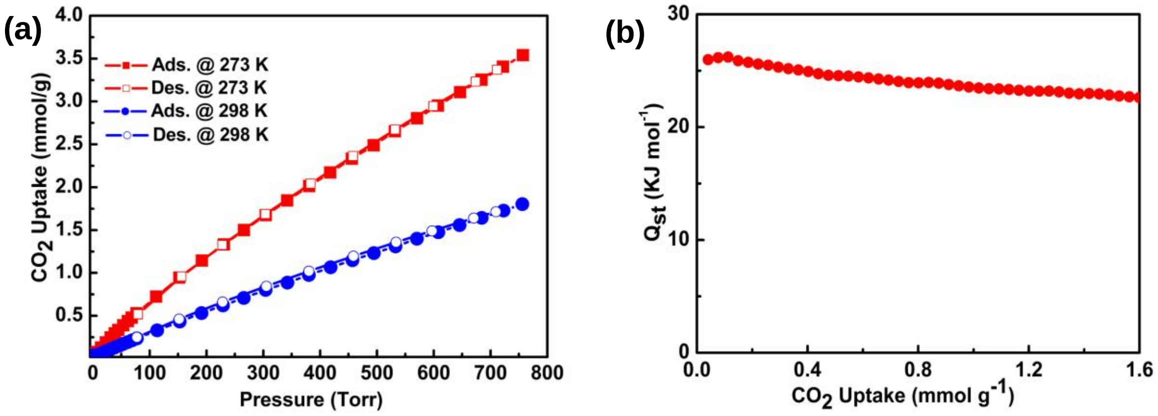

**Fig. S11.** (a) Methane adsorption isotherm on **JLU-Liu2** at 273 K (green) and 298 K (magenta). Adsorption and desorption branches are shown with closed and open symbols, respectively. (b) Isosteric heat of adsorption for $CH_4$ in **JLU-Liu2**.

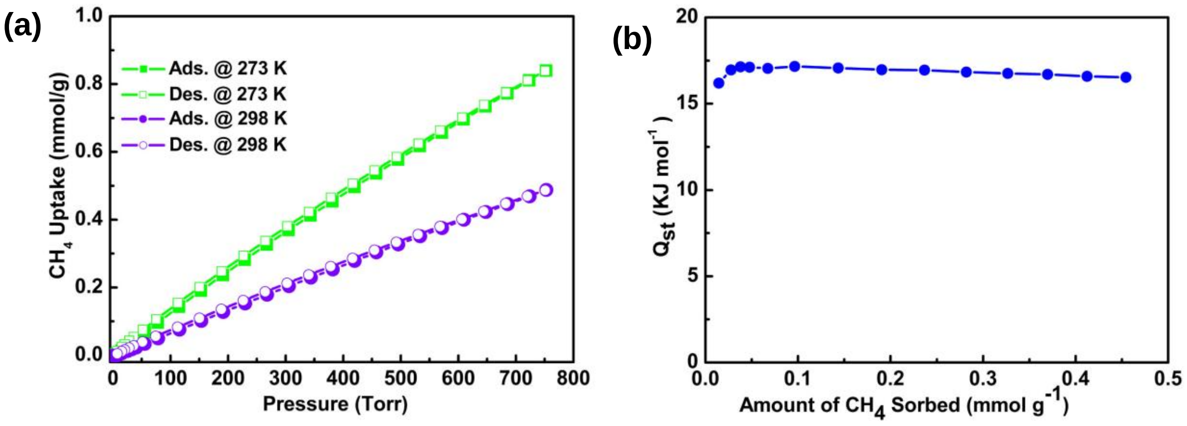

**JLU-Liu-2** can also adsorb a certain amount of $CH_4$ at 273 K and at 298 K reached 18.8 and 10.9 $cm^3/g$ (0.84 and 0.49 mmol/g). We determined the initial slopes in the Henry region of the adsorption isotherms of **JLU-Liu2**. The ratios of the slopes were used to estimate the sorption selectivities for $CO_2$ over $CH_4$. From these data, the $CO_2/CH_4$ selectivity is 9:1 at 273 K and 4:1 at 298 K.

**Fig. S12.** Calculation of $CO_2$:$CH_4$ selectivity by initial slope of the gas uptake on **JLU-Liu2** at 273K (a) and 298K (b). (red and blue liner: uptake of $CO_2$, green and purple liner: uptake of $CH_4$, solid line: liner fitted data).

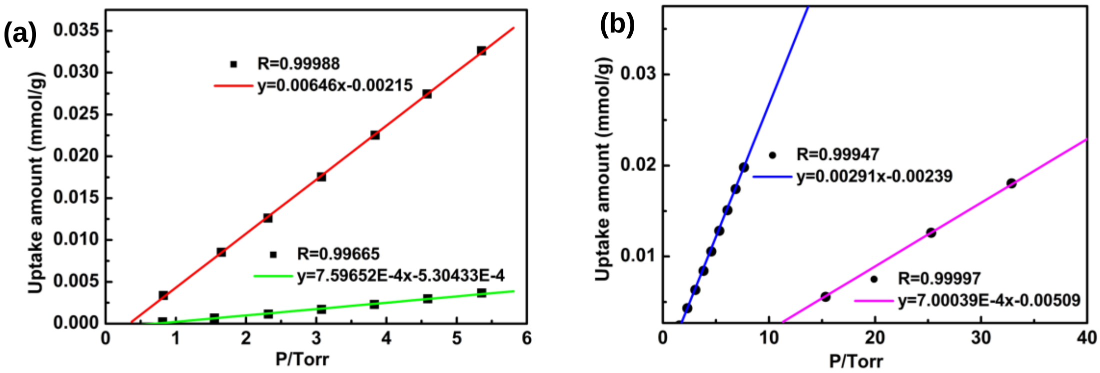

**Fig. S13.** The powder X-ray diffraction pattern of grafted **JLU-Liu2-en** is well matched with calculated **JLU-Liu2**, show that preservation of the framework structure.

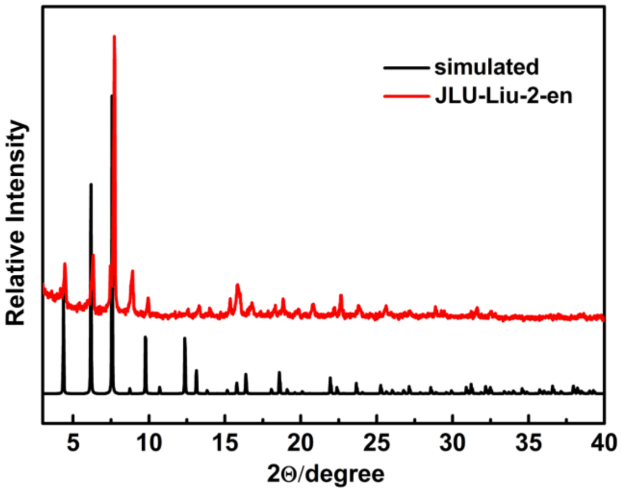

**Fig. S14.** Infrared spectra compared with **JLU-Liu2** and **JLU-Liu2-en** (4000-400 cm$^{-1}$).

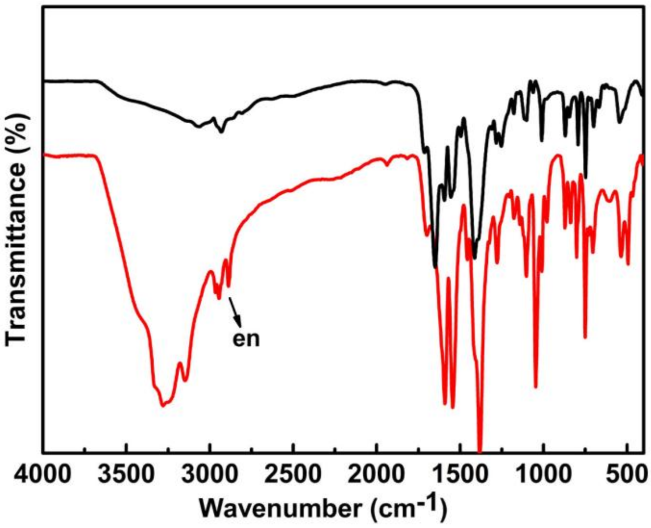

A sample of **JLU-Liu2** (60mg) was soaked in 5 mL of anhydrous toluene, an excess amount of ethylenediamine (en) was added. The suspension was settled under 65 $^{o}$C to optimize the extent of grafting. The product promoting color changed from green to blue and washed with n-hexane to remove the unreacted en, and then dried under reduced pressure to obtain amine-functionalized product **JLU-Liu2-en**. The powder X-ray diffraction pattern of grafted **JLU-Liu2-en** is similar to that of **JLU-Liu2**, indicating the stability of the framework structure after en grafting. The IR spectrum of **JLU-Liu2-en** compared with **JLU-Liu2** provides further demonstration for en grafting, the $\nu_{NH}$ and $\nu_{CH}$ stretching vibrations were observed in **JLU-Liu2-en**, $\nu_{CH}$ (2887 and 2947 cm$^{-1}$) bands shift to a higher energies show that en is coordinated to a Lewis acid. Indeed, compared with the $N_2$ adsorption data of **JLU-Liu2** and **JLU-Liu2-en**, the BET surface area reduced to 1157 m$^2$/g after grafting. The pore size distribution curves indicate that the en grafting leads to a slight decrease of the pore sizes.

**Fig. S15.** Nitrogen sorption isotherms on **JLU-Liu2-en** at 77 K and pore size distribution analysis. Adsorption and desorption branches are shown with closed and open symbols, respectively.

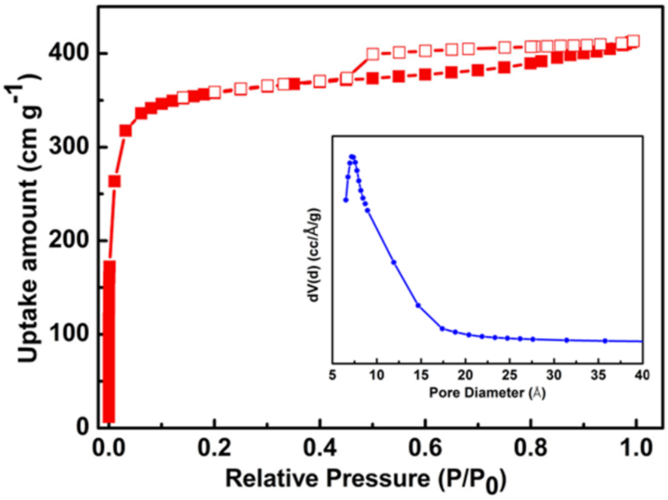

**Fig. S16.** Isosteric heat of adsorption for $CO_2$ in **JLU-Liu2** (red) and **JLU-Liu2-en** (blue).

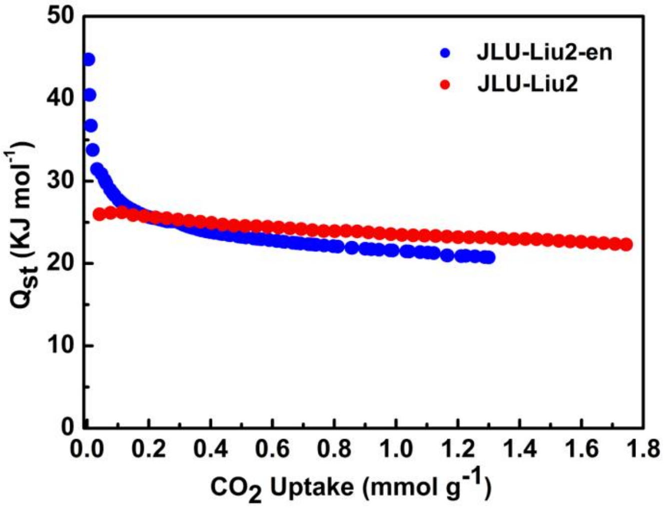

**Fig. S17.** Adsorption isotherm of different solvent vapors on **JLU-Liu2** at 298 K. Color scheme: benzene (red), toluene (green), *p*-xylene (black), methanol (blue) and cyclohexane (cyan).

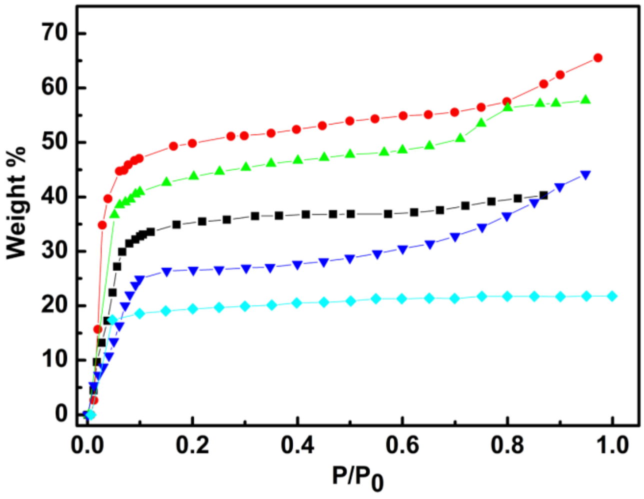

Recently, an increasing number of studies have been tried to incorporate RhB (Rhodamine B) into hybrid organic–inorganic materials for applications in fields such as solid-state lasing, optical filters, and optoelectronics.[8] RhB, with the smaller size (14.537 × 7.552 Å$^2$) compared to the square shaped channel of **JLU-Liu2** (diameter of 16.7 × 16.7 Å$^2$) and the anionic character, could freely diffuse into the large channels of **JLU-Liu2**. Electrostatic interactions between the cationic RhB and the negatively charged framework of the **JLU-Liu2** preclude further diffusion of RhB out of the cavities once encapsulated. **JLU-Liu2** was assembled with RhB dye molecules by soaking **JLU-Liu2** in solutions of RhB in ethanol for 36 h, promoting color changed from green to rose. Figure S18 shows the fluorescence spectra for **JLU-Liu2-RhB**. Clearly, **JLU-Liu2-RhB** display intensive luminescence emissions peak at 607 nm with the excitation peak at 466 nm at room temperature. The blue shift of **JLU-Liu2-RhB** compared to **JLU-Liu-2** may be attributed to the interaction between RhB and the framework of **JLU-Liu-2**.

**Fig. S18.** Luminescent spectra of activated **JLU-Liu2** and **JLU-Liu2-RhB** when excited at 466 nm.

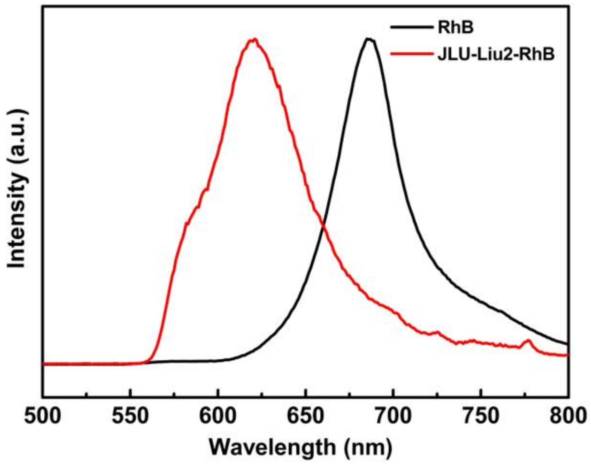

**Fig. S19.** Temperature dependence of the $\chi_M$T value and reciprocal susceptibility $\chi_M^{-1}$ for **JLU-Liu2**.

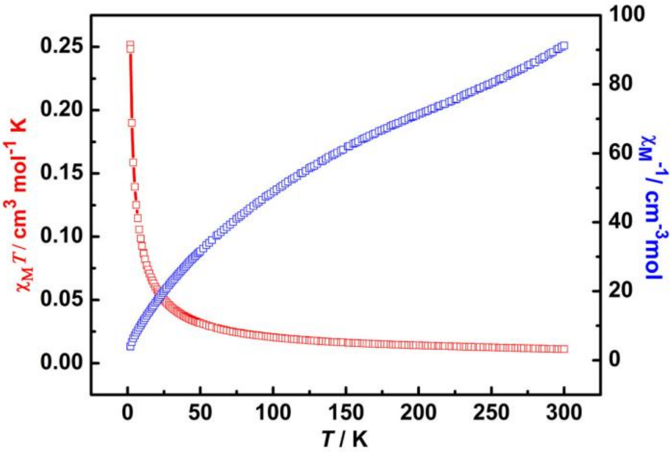

**X-ray Crystallography for JLU-Liu2.**

Data was performed on a Rigaku RAXIS-RAPID IP diffractometer by using graphite-monochromated Mo-Kα radiation (λ = 0.71073 Å). The CCDC-947595 containing the supplementary crystallographic data for this paper can be obtained free of charge from the Cambridge Crystallographic Data Centre via www.ccdc.cam.ac.uk/data_request/cif. Space groups were determined using XPREP implemented in APEX2.[9] Structure was solved using SHELXS-97 (direct methods) and refined using SHELXL-97 (full-matrix least-squares on $F^2$). For **JLU-Liu2** the ligand moiety was disordered and atoms were refined using geometry restraints. Restraints were also used to refine anisotropic displacement parameters of disordered atoms. Disordered solvent molecules were refined isotropically. Hydrogen atoms were placed in appropriate positions. The DMF and water molecules were highly disordered and could not be modeled properly, thus the SQUEEZE routine of PLATON was applied to remove the contributions to the scattering from the solvent molecules. The reported refinements are of the guest-free structures using the *.hkp files produced using the SQUEEZE routine. Additional details are presented in Table S1.

**Table S1.** Crystal data and structure refinement for **JLU-Liu2**

| **Compound** | **JLU-Liu2** |
|---|---|
| Empirical formula | $C_{38}H_{47}ClCu_4N_{18}O_{18}$ |
| Formula weight | 1333.55 |
| Temperature (K) | 293(2) |
| Wavelength (Å) | 0.71073 |
| Crystal system | Cubic |
| Space group | *P*m-3m |
| *a* (Å) | 20.208(2) |
| α (deg) | 90 |
| Volume (Å$^3$) | 8252.0(16) |
| Z | 3 |
| Dcalc (Mg/m$^3$) | 0.804 |
| Absorption coefficient (mm$^{-1}$) | 0.832 |
| F(000) | 2034 |
| Crystal size (mm) | 0.27 × 0.26 × 0.25 |
| Theta range for data collection | 3.02 to 27.43 deg. |
| Goodness-of-fit on $F^2$ | 1.145 |
| Final R indices [$I>2\sigma(I)$] | $R_1$ = 0.0736, w$R_2$ = 0.2069 |
| R indices (all data) | $R_1$ = 0.0842, w$R_2$ = 0.2151 |

$R_1=\sum||F_o|-|F_c||/\sum|F_o|$. $wR_2=[\sum[w(F_o^2-F_c^2)^2]/\sum[w(F_o^2)^2]]^{1/2}$

**Table S2.** Summary of MOFs based on $[M_4Cl]^{7+}$ square with sodalite-like cage: Sodalite cage sizes, porosities, and isosteric heats of Cu-BTC, Mn/Fe/Cu-BTT, Cu-TPB, Mn/Cu-TPT, Cu-BTTri, Cu-TTCA and the en-Cu-BTTri. Data are taken from Refs. [1-7].

| | **Cu-BTC Ref.1** | **Cu-BTC Ref.2** | **Mn/Fe/Cu -BTT** | **Cu-TPB Mn/Cu-TPT** | **Cu-BTTri** | **en-Cu-BTTri** | **Cu-TTCA** | **JLU-Liu2** | **JLU-Liu2-en** |
|---|---|---|---|---|---|---|---|---|---|
| **Small sod cage size (Å)** | 15.4 | 15.4 | 19 | 29.1 | 19 | - | 20.7 | 20.2 | - |
| **Big sod cage size (Å)** | 18.2 | 18.2 | 23 | 37.3 | 23 | - | 29.3 | 28 | - |
| **BET SA [m$^2$ g$^{-1}$]** | 572 | 789.1 | 2100/2010/1710 | 1120/1580 | 1770 | 345 | 1680 | 2330 | 1157 |
| **Pore volume[cm$^3$ g$^{-1}$]** | 0.39 | 0.341 | - | - | - | - | 0.639 | 0.87 | 0.44 |
| **$H_2$ uptake[wt%] (77K)** | - | 1.5 | 2.25/2.3/2.42 | - | 1.7 | - | 0.91 | 1.54 | - |
| **$Q$st ($H_2$) [KJ mol$^{-1}$]** | - | 6.83 | 10.6/13.1/9.4 | 8.2/7.6 | 6.1 | - | 3.38 | 7.37 | - |
| **$CO_2$ uptake [mmol g$^{-1}$]** | - | 5.53/3.26 | - | - | 3.24 | 1.27 | 15.7(195K) | 3.53 /1.86 | 2.54/1.30 |
| **$Q_{st}$($CO_2$) [KJ mol$^{-1}$]** | - | 25.38 | - | - | 21 | 90 | - | 26 | 45 |

## References

[1] F.-J. Ma, S.-X. Liu, C.-Y. Sun, D.-D. Liang, G.-J. Ren, F. Wei, Y.-G. Chen and Z.-M. Su, *J. Am. Chem. Soc.*, 2011, **133**, 4178-4181.

[2] Y.-X. Tan, Y.-P. He and J. Zhang, *Chem. Comm.*, 2011, 47, 10647-10649.

[3] (*a*) M. Dincă, A. Dailly, Y. Liu, C. M. Brown, D. A. Neumann and J. R. Long, *J. Am. Chem. Soc.*, 2006, **128**, 16876-16883; (*b*) M. Dincă, W. S Han, Y. Liu, A. Dailly, C. M. Brown and J. R. Long, *Angew. Chem., Int. Ed.*, 2007, **46**, 1419-1422.

[4] A. Demessence, D. M. D'Alessandro, M. L. Foo and J. R. Long, *J. Am. Chem. Soc.*, 2009, **131**, 8784-8786.

[5] T. M. McDonald, D. M. D'Alessandro, R. Krishna and J. R. Long, *Chem. Sci.* 2011, **2**, 2022-2028.

[6] Y.-N. Gong, M. Meng, D.-C. Zhong, Y.-L. Huang, L. Jiang and T.-B. Lu, *Chem. Commun.*, 2012, **48**, 12002-12004.

[7] M. Dinca, A. Dailly, C. Tsay and J. R. Long, *Inorg. Chem.*, 2007, **47**, 11-13.

[8] P. Yang, G. Wirnsberger, H. C. Huang, S. R. Cordero, M. D. McGehee, B. Scott, T. Deng, G. M. Whitesides, B. F. Chmelka, S. K. Buratto and G. D. Stucky, *Science*, 2000, **287**, 465-467.

[9] Bruker APEX2; Bruker AXS, Inc.: Madison, WI, 2010.